arXiv:cond-mat/0504686v1 [cond-mat.other] 26 Apr 2005

Disorder Potentials near Lithographically Fabricated Atom Chips

P. Krüger,[1,*] L. M. Andersson,[1] S. Wildermuth,[1] S. Hofferberth,[1]
E. Haller,[1] S. Aigner,[1] S. Groth,[1] I. Bar-Joseph,[2] and J. Schmiedmayer[1]

[1]*Physikalisches Institut, Universität Heidelberg, 69120 Heidelberg, Germany*
[2]*Department of Condensed Matter Physics, The Weizmann Institute of Science, Rehovot 76100, Israel*

(Dated: September 24, 2004)

We show that previously observed large disorder potentials in magnetic microtraps for neutral atoms are reduced by about two orders of magnitude when using atom chips with lithographically fabricated high quality gold layers. Using one dimensional Bose-Einstein condensates, we probe the remaining magnetic field variations at surface distances down to a few microns. Measurements on a 100 μm wide wire imply that residual variations of the current flow result from *local* properties of the wire.

PACS numbers: 39.90.+d, 03.75.Be

Trapping and manipulating cold neutral atoms in microtraps near surfaces of atom chips is a promising approach towards a full quantum control of matter waves on small scales [1]. In a number of experiments a variety of trapping, guiding and transporting potentials have been realized using current carrying wires [2, 3, 4, 5, 6, 7, 8], atom manipulation with electric fields was integrated on an atom chip [9], coherent dynamics of internal atomic hyperfine states was observed [10] and easy formation of Bose-Einstein condensates (BEC) was demonstrated [11, 12, 13, 14].

The full potential of atom chip experiments is only accessible if the potentials can be miniaturized to a scale of typically 1 μm or below where appreciable tunnelling rates between separated traps can be reached, and efficient atom-atom coupling between atoms in neighboring trap sites [15] can be achieved. While the fabrication of structure sizes < 1 μm is not problematic, unintended potential roughness has been reported to severely alter the trapping at surface distances d below ~ 100 μm, resulting in a longitudinal fragmentation of elongated clouds [16, 17, 18, 19]. Such disorder potentials have been observed near macroscopic wires and atom chips fabricated by electroplating techniques [20, 21, 22].

Strongly confining trapping and guiding potentials on atom chips are formed by the subtraction of two magnetic fields, the field of a current carrying wire and a (homogeneous) bias field (side guide configuration [23]). The remaining field at the potential minimum is determined by the angle between wire field and bias field. A small change of the current direction may result in a significant change in the trapping potential.

The observed disorder potentials have been attributed to inhomogeneous magnetic field components ΔB in the direction *parallel* to the current carrying wire creating the trapping field B [16, 17, 18, 19]. It has been suggested that such field components could be derived from fabrication inhomogeneities, surface roughness [24, 25] and residual roughness of the wire borders [26]. The model of Wang et al. [26] provides a full quantitative explanation of the potentials found near electroplated gold wires [19].

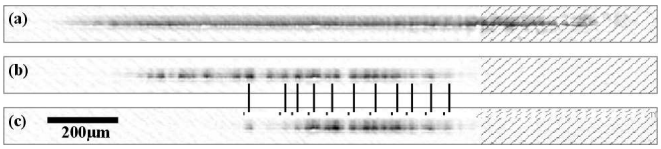

FIG. 1: *In situ* absorption images of atom clouds positioned at a chip surface distance of ~ 5 μm above a current carrying wire (cross section 3.1×10 μm^2). Parts of the images do not fully represent the atom density distribution since the imaging light beam was obstructed by bonding wires (hatched regions). a) Thermal atoms show no fragmentation. b) BECs display a much higher sensitivity and residual disorder potentials cause a fragmentation of the cloud. c) A longitudinal displacement of the BEC by tuning the trapping potential shows that the disorder potential is stable in position.

In this Letter, we report on a dramatic reduction of the disorder potentials in our experiments. For cold thermal atoms ($T \sim 1$ μK) we do not observe fragmentation of the trapped clouds even when they are brought to distances of 3 μm from the surface of a current carrying wire. Yet, we are able to measure a small residual potential roughness near the wire by creating BECs close to the surface (Fig. 1).

We attribute this reduction of the disorder potentials to our atom chip fabrication method. We obtain chips with very smooth wire structures by adapting a standard microchip fabrication process to the production of our atom chips [27, 28]. Masks written by electron beam lithography are used to structure a several micron thick, high quality gold layer on a semiconductor wafer using a lift-off procedure. The result is a smooth gold mirror with precise gaps defining the current path in the wire [1, 7, 27]. Fig. 2 shows electron microscope images of the gold surface and the wire edges.

In our experiment, more than 10^8 ^{87}Rb atoms are accumulated a few mm from the chip surface which serves directly as a mirror for a reflection magneto-optical trap (MOT) [2]. These atoms are subsequently transferred to

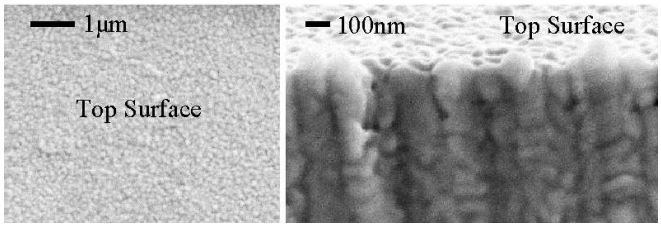

FIG. 2: Scanning electron microscope images of the chip wire surface (left) and edges (right). The grain sizes of < 100 nm determine both the surface and edge roughness.

a purely magnetic trap and cooled to ~ 5 μK by radio frequency (RF) evaporation. Both the MOT and the magnetic trap are based on copper wire structures mounted directly underneath the chip [29]. The resulting sample of $\gtrsim 10^6$ atoms is then loaded to the selected chip trap and location, where a second stage of RF evaporative cooling creates either a BEC or thermal cloud just above the critical condensation temperature.

We image the atomic clouds near the surface *in situ* by resonant absorption imaging with ~ 3.5 μm resolution. In order to determine the cloud's distance from the surface d, we slightly incline the imaging light with respect to the chip mirror surface by ~ 25 mrad. For sufficiently small d (< 100 μm) this leads to a duplicated absorption image [14] (Fig. 3).

While the wire currents are very well known, the strength of the external bias fields has to be calibrated with measurements of d at sufficiently large d. As our imaging resolution does not allow to measure d for very close surface approaches, we use the calibrated values of the bias fields together with the measured wire currents to infer d in these cases.

We have probed the residual potential roughness for various trapping geometries based on a 100 μm and several 10 μm wide wires at atom-surface distances down to 3 μm. The global parameters of the atomic cloud like atom number and temperature are determined by the ballistic expansion of the cloud in time-of-flight measurements.

With thermal atoms we always observe smooth longitudinal absorption profiles inside the trap (Fig. 1a), independent of the wire used to form the trap and the position of the atomic cloud. For the closest approach of $d = 3$ μm, a cloud at $T = 1$ μK remains un-fragmented within our detection resolution, even when summing up many realizations of the experiment to reduce measurement noise. Assuming that the atomic density profile follows the Boltzmann distribution $n \sim \exp(-V/k_B T)$, we can put an upper limit to the residual magnetic field roughness $\Delta B/B < 2 \times 10^{-4}$ where B is the field produced by the wire at that distance.

BECs are a much more sensitive probe of potential roughness. The relevant energy scale, given by the chemical potential μ, can be orders of magnitude smaller than the temperature of thermal atoms. Figs. 1b and c show typical absorption images of fragmented BECs at $d = 5$ μm from one of the 10 μm wide wires. Altering the longitudinal confinement by varying the current in an independent auxiliary wire leads only to an overall displacement of the cloud while the local disorder potential variations remain stable in their positions. Over many months of experiments no change was observed in the position of the fragments.

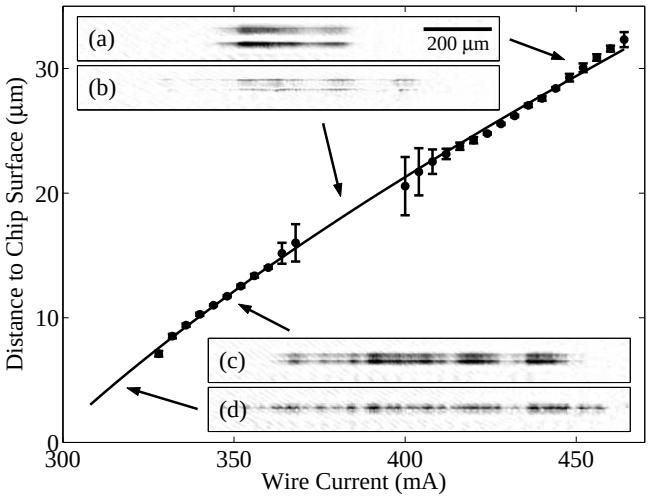

FIG. 3: Distance d of the BEC from the (mirror) chip surface as a function of wire current (3.1×100 μm^2 wire). Atoms near the surface produce a double image when illuminated by an inclined imaging beam as shown in the inserts a)-c). The imaging beam together with the chip surface produces a fringe pattern that makes distance measurements less reliable for certain surface distances (b). For clouds closer than ~ 5 μm from the surface, the two images merge (d). To determine d also in these cases we use an extrapolation according to a best fit (solid line) with the exact bias field strength as only fitting parameter. The fitting model takes the finite size of the wire into account.

The inserts of Fig. 3 show absorption profiles of BECs at various heights d above the 100 μm wide wire. As the surface is approached, the longitudinal trapping potential becomes flatter, thus the BECs extend over a longer stretch of the wire. As d is increased, the strength of the disorder potentials is reduced and the typical length scale of fragmentation increases. For $d \gtrsim 30$ μm, virtually no fragmentation is detected, even with a BEC.

For a quantitative analysis, we extract longitudinal density profiles $n_{1\mathrm{d}}$ from the *in situ* absorption images and calibrate them with the absolute atom number derived from time-of-flight images taken under equal experimental conditions. For $n_{1\mathrm{d}} \lesssim 100$ μm^{-1} (^{87}Rb atoms), the confinement is of one dimensional (1d) character, i.e. the transverse single particle ground state energy exceeds the chemical potential μ of the BEC. In our experiments this condition is always fulfilled, and the actual potential

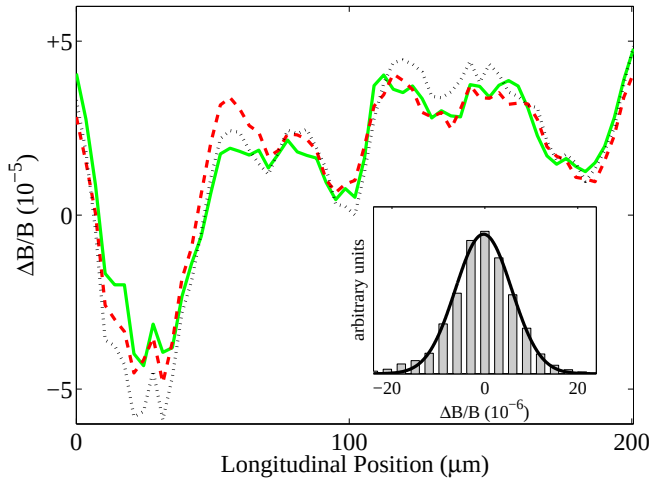

FIG. 4: (color online) Longitudinal potential profiles measured with BECs at a constant distance of $d = 10$ μm from the surface of the 100 μm broad wire. The different traces were measured at different currents and are normalized to the respective trapping fields. The bias field (10 G, 20 G, 30 G; black dotted, solid green, dashed red lines, respectively) was adapted in order to keep d constant. The insert shows a histogram of the deviations of the curves. The width of the distribution ($\sigma \sim 8 \times 10^{-6}$) is similar to the shot to shot variations of different realizations of the same experiment with equal wire currents.

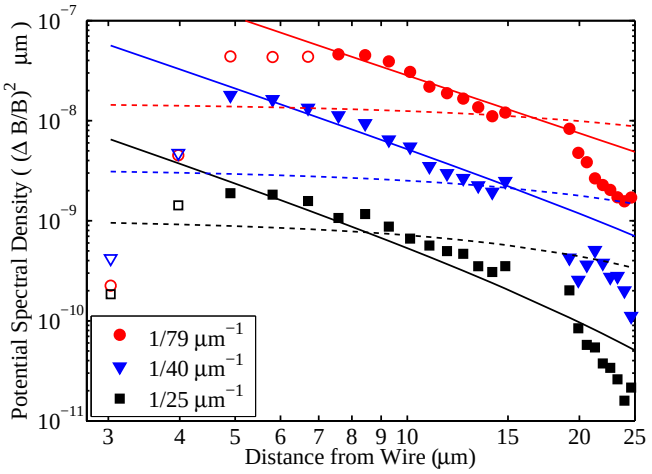

FIG. 5: (color online) Spectral power density of the disorder potentials near the 100 μm wide wire for three spatial frequencies. The open symbols correspond to data where the detected signal is limited by the chemical potential μ of the BEC. For these data points the complete depth of the potential cannot be measured, and they were omitted in the analysis. The solid lines are best fits according to a local fluctuating current path model, the dashed lines show best fits to the model outlined in [26]. For both models the only fitting parameter is the strength of current path fluctuation at the respective spatial frequency k.

experienced by the atoms can be reconstructed according to $V(x) = -2\hbar\omega_\perp a_{\rm scat} n_{\rm 1d}(x)$ where $a_{\rm scat} \approx 5.6$ nm is the ^{87}Rb scattering length. This expression is derived under the assumption of a constant (global) μ in a 1d Thomas-Fermi (TF) approximation [30]. This is strictly valid only in an equilibrium state of the system. This may not be the case in our experiment over the entire length of the BEC (~ 1 mm). Similar to the observations previously made in an optical dipole double well potential [31], a variation of μ on longitudinal length scales > 200 μm is maintained longer than the life time of the BEC if strong potential barriers separate the different fragments of the condensate. We have confirmed the validity of the TF-approach for shorter wavelength components by monitoring the $n_{\rm 1d}(x)$ profile over the entire lifetime of the condensate. We observe that the reconstructed potential fluctuations at wavelengths $\lesssim 200$ μm remain constant. We limit the further analysis to length scales shorter than 200 μm.

To assess whether the observed disorder potentials are magnetic in origin we have varied the wire current while adapting the bias field so that the BECs were trapped at fixed distances from the wire. Magnetic disorder potentials stemming from an irregular current flow should scale linearly with the current in the wire I. Figure 4 shows an example of relative potential variations $\Delta B/B$ reconstructed from BECs positioned at $d = 10$ μm for three different currents. To quantify the consistency between the measurements, we compare the shot to shot variations of $\Delta B/B$ with equal currents to those with different currents. We find equal widths of the residual differences between the graphs. We conclude that within the statistical similarity of the $\Delta B/B$ distributions ($\sim 3 \times 10^{-6}$), we can exclude any current independent sources of disorder potentials such as electrostatic patch effects [32] at the scale of 10^{-13} eV for $d > 5$ μm.

In order to study the source of the irregular current flow we have measured the variation of the disorder potentials with d. Wires of two different widths, 10 μm and 100 μm, were used. The main observation is that the scaling of the amplitude and the frequency spectrum of the disorder potentials with d for the two wires are very similar. For $d < 50$ μm this would not be the case if edge fluctuations were dominating as can be derived from the edge fluctuation model [26].

For the 100 μm wide wire, Fig. 5 shows potential spectral densities (PSD) of the disorder potential at three different spatial frequencies k. In the examined d-range, the potentials scale more strongly with d than they would for dominating edge fluctuations [26] for all frequency components. We interpret the clear difference in slope of the experimental data and the wire edge model as an indication that *local* current path deviations are important. Such deviations can occur due to inhomogeneous conductivity or top surface roughness [24, 25].

The simplest model taking local sources of current path deviations into account is a current flowing along a nar-

row irregular path below the atoms [33]. Such a model gives reasonable agreement in the slope of the PSD as d is increased as can be expected as long as d is small compared to the relevant period $1/k$. Applying this method over the full spectrum ($k > 1/200\ \mu\mathrm{m}^{-1}$), we obtain a local current flow fluctuation spectrum that scales as $\sim 1/k^2$. Microscopically well characterized wires will have to be fabricated and tested to develop a more refined model explaining the disorder potentials caused by local current deviations.

From our data and the simple local model we can estimate the rms strength of the relative disorder potential and scale it to different heights. At a surface distance of $d = 10\ \mu$m we find the rms $\Delta B/B = 3 \times 10^{-5}$ ($< 10^{-5}$) for spatial frequencies $k > 1/200\,\mu\mathrm{m}^{-1}$ ($k > 1/50\,\mu\mathrm{m}^{-1}$). At $d > 30\ \mu$m, where disorder potentials near electroplated wires have been measured, $\Delta B/B$ is significantly smaller than the measurement sensitivity in our case (5×10^{-6}). This corresponds to a reduction by about two orders of magnitude.

To conclude, we have investigated magnetic disorder potentials near lithographically fabricated current carrying wires using quasi 1d BECs. The measured potentials are orders of magnitude smaller than previously observed in other atom chip experiments, which we attribute to our different chip fabrication method resulting in much smoother and much more homogeneous wires. We have strong evidence that the remaining potential roughness can be attributed to deviations of the current flow from its nominal path through the wire. We find that in addition to wire edge roughness *local* fluctuations can be a dominating source of the disorder potentials. Our method has a sensitivity for $\Delta B/B$ of better than 10^{-5} for a single point measurement, corresponding to a deviation of the local current path smaller than 10^{-5} rad. The strong scaling of the magnetic field fluctuations with spatial frequency indicates a dominance of large scale inhomogeneities which can be dealt with by improving the fabrication. The smallness of high frequency fluctuations opens up the way to μm scale quantum manipulation on atom chips.

We thank M. Brajdic and L. Della Pietra for help in the experiments. This work was supported by the European Union, contract numbers IST-2001-38863 (ACQP), HPRN-CT-2002-00304 (FASTNet), HPMF-CT-2002-02022, and HPRI-CT-1999-00114 (LSF) and the Deutsche Forschungsgemeinschaft, contract number SCHM 1599/1-1.

* Electronic address: krueger@physi.uni-heidelberg.de; URL: `http://www.atomchip.net`

[1] R. Folman, P. Krüger, J. Schmiedmayer, J. Denschlag, and C. Henkel, Adv. At. Mol. Opt. Phys. **48**, 263 (2002).
[2] J. Reichel, W. Hänsel, and T. W. Hänsch, Phys. Rev. Lett. **83**, 3398 (1999).
[3] W. Hänsel, J. Reichel, P. Hommelhoff, and T. W. Hänsch, Phys. Rev. A **64**, 063607 (2001).
[4] J. Reichel, Appl. Phys. B **74**, 469 (2002).
[5] D. Müller, D. Z. Anderson, R. J. Grow, P. D. D. Schwindt, and E. A. Cornell, Phys. Rev. Lett. **83**, 5194 (1999).
[6] N. H. Dekker *et al.*, Phys. Rev. Lett. **84**, 1124 (2000).
[7] R. Folman, P. Krüger, D. Cassettari, B. Hessmo, T. Maier, and J. Schmiedmayer, Phys. Rev. Lett. **84**, 4749 (2000).
[8] D. Cassettari, B. Hessmo, R. Folman, T. Maier, and J. Schmiedmayer, Phys. Rev. Lett. **85**, 5483 (2000).
[9] P. Krüger *et al.*, Phys. Rev. Lett. **91**, 233201 (2003).
[10] P. Treutlein, P. Hommelhoff, T. Steinmetz, T. W. Hänsch, and J. Reichel, Phys. Rev. Lett. **92**, 203005 (2004).
[11] H. Ott, J. Fortagh, G. Schlotterbeck, A. Grossmann, and C. Zimmermann, Phys. Rev. Lett. **87**, 230401 (2001).
[12] W. Hänsel, P. Hommelhoff, T. W. Hänsch, and J. Reichel, Nature **413**, 498 (2001).
[13] A. E. Leanhardt *et al.*, Phys. Rev. Lett. **89**, 040401 (2002).
[14] S. Schneider *et al.*, Phys. Rev. A **67**, 023612 (2003).
[15] T. Calarco, E. A. Hinds, D. Jaksch, J. Schmiedmayer, J. I. Cirac, and P. Zoller, Phys. Rev. A **61**, 022304 (2000).
[16] J. Fortagh, H. Ott, S. Kraft, A. Günther, and C. Zimmermann, Phys. Rev. A **66**, 041604(R) (2002).
[17] A. E. Leanhardt, Y. Shin, A. P. Chikkatur, D. Kielpinski, W. Ketterle, and D. E. Pritchard, Phys. Rev. Lett. **90**, 100404 (2003).
[18] M. P. A. Jones, C. J. Vale, D. Sahagun, B. V. Hall, and E. A. Hinds, Phys. Rev. Lett. **91**, 080401 (2003).
[19] J. Estève *et al.*, (2004), physics/0403020.
[20] M. Drndić, K. S. Johnson, J. H. Thywissen, M. Prentiss, and R. M. Westervelt, Appl. Phys. Lett. **72**, 2906 (1998).
[21] J. Fortagh, H. Ott, G. Schlotterbeck, C. Zimmermann, B. Herzog, and D. Wharam, Appl. Phys. Lett. **81**, 1146 (2002).
[22] B. Lev, Quant. Inf. Comp. **3**, 450 (2003).
[23] J. Denschlag, D. Cassettari, and J. Schmiedmayer, Phys. Rev. Lett. **82**, 2014 (1999).
[24] A. Kasper *et al.*, J. Opt. B **5**, S143 (2003).
[25] T. Schumm *et al.*, (2004), physics/0407094.
[26] D.-W. Wang, M. D. Lukin, and E. Demler, Phys. Rev. Lett. **92**, 076802 (2004).
[27] S. Groth *et al.*, Appl. Phys. Lett. (2004), in press, cond-mat/0404141.
[28] This fabrication method [27] was used for the chip in all our previous experiments [7, 8, 9].
[29] S. Wildermuth *et al.*, Phys. Rev. A **69**, 030901(R) (2004).
[30] T. Bergeman, M. G. Moore, and M. Olshanii, Phys. Rev. Lett. **91**, 163201 (2003).
[31] Y. Shin *et al.*, Phys. Rev. Lett. **92**, 150401 (2004).
[32] J. M. McGuirk, D. M. Harber, J. M. Obrecht, and E. A. Cornell, Phys. Rev. A **69**, 062905 (2004).
[33] This is equivalent to using the wire edge model mentioned above but with a very small wire width and equal current.